Soil Dynamics and Earthquake Engineering 29 (2009) 710–721

Contents lists available at ScienceDirect

Soil Dynamics and Earthquake Engineering

journal homepage: www.elsevier.com/locate/soildyn

Site response to multi-directional earthquake loading: A practical procedure

J. Yang *, X.R. Yan

Department of Civil Engineering, The University of Hong Kong, Hong Kong

ARTICLE INFO

Article history:
Received 23 July 2008
Accepted 28 July 2008

Keywords:
Site response
Vertical ground motion
Horizontal ground motion
Soil nonlinearity

ABSTRACT

Site response to earthquake loading is one of the fundamental problems in geotechnical earthquake engineering. Most site response analyses assume vertically propagating shear waves in a horizontally layered soil–rock system and simply ignore the effect of site response to vertical earthquake motion, although actual ground motions are comprised of both horizontal and vertical components. In several recent earthquakes very strong vertical ground motions have been recorded, raising great concern over the potential effect of vertical motion on engineering structures. Being a step toward addressing this concern, this paper presents a simple and practical procedure for analysis of site response to both horizontal and vertical earthquake motions. The procedure involves the use of the dynamic stiffness matrix method and equivalent-linear approach, and is built in the modern MATLAB environment to take full advantages of the matrix operations in MATLAB. The input motions can be specified at the soil–bedrock interface or at a rock outcropping. A detailed assessment of the procedure is given, which shows that the procedure is able to produce acceptable predictions of both vertical and horizontal site responses.

1. Introduction

Characteristics of earthquake ground motions at a given site are strongly influenced by site conditions such as subsurface soil properties and stratigraphy. This site effect is commonly known as soil amplification although the name may be misleading, since there is in fact amplification in certain range of frequencies and deamplification in others. Evaluation of site response is one of the crucial problems in earthquake engineering. Practicing engineers rely on the response analysis to predict ground surface motions and dynamic stresses and strains in the ground, which are important information for seismic design of various superstructures and underground facilities.

SHAKE [1] is among the first computer programs developed for the purpose of ground response analysis. This program is based on the one-dimensional wave propagation theory and computes the response of a horizontally layered soil–rock system to vertically traveling shear waves using a recursive algorithm. The nonlinear behaviour of soils during earthquake excitation is modeled through an iterative equivalent-linear approach. Over the past three decades, a number of procedures and computer programs of various sophistications, such as truly nonlinear modelling in time domain and fully coupled liquefaction analysis (e.g. see [2]), have been developed for ground response analysis. Nevertheless, SHAKE, with its latest version known as SHAKE91 [3], appears to remain most popular in practical applications. This may be due primarily to its simplicity in modelling and acceptable predictive performance. In recent years, useful efforts have been put into modification of SHAKE by using some modern development platforms such that it is more user-friendly [4,5]. These newly developed computer programs essentially follow the same concept and formulation as SHAKE.

During an earthquake the site in question is not only subjected to horizontal shaking, but also to vertical vibration. Site response to vertical earthquake motion, compared with that to the horizontal shaking, appears to have received much less attention. Current practice has tended to focus on the effect of horizontal motion and simply disregard the vertical component. This practice is partly due to the consideration that engineering structures have adequate resistance to dynamic forces induced by the vertical ground motion, which is generally smaller in magnitude and richer in high frequencies than its horizontal counterpart. If the effect of vertical motion is explicitly included in earthquake-resistant design, it is typically assumed that the ratio of vertical to horizontal (V/H) response spectra will not exceed two-thirds over the range of periods of interest [6]. In the pseudostatic analyses, the peak vertical acceleration is usually assumed to be a half or two-thirds of the peak horizontal acceleration [7].

It is worth noting, however, that very strong vertical ground motions have been repeatedly recorded in recent earthquake

* Corresponding author.
E-mail address: junyang@hku.hk (J. Yang).

0267-7261/$ - see front matter © 2008 Elsevier Ltd. All rights reserved.
doi:10.1016/j.soildyn.2008.07.008

Nomenclature

h_m	thickness of soil layer, m
E	Young's modulus of soil
E_c,E^*_c	constrained modulus and complex constrained modulus of soil
G,G^*	shear modulus and complex shear modulus of soil
k,$\tilde{k}$	complex wave numbers of horizontal and vertical motion respectively
N_m,N_{m+1}	normal forces at tops of layer m and m+1
t	time
T_m,T_{m+1}	shear forces at tops of layer m and m+1
$TR_{m,n}$	Transfer function between layer n and layer m
u	horizontal displacement
U	amplitude of horizontal displacement
v_s,v_p	shear wave velocity and compressional wave velocity, respectively
w	vertical displacement
W	amplitude of vertical displacement
z	depth
α	complex impedance ratio for horizontal motion
ζ,$\tilde{\zeta}$	damping ratios of soil for horizontal and vertical motion, respectively
$\tilde{\eta}$	viscosity coefficient for vertical motion
ρ	mass density of soil
υ	Poisson's ratio of soil
ω	circular frequency

events. For example, the vertical acceleration recorded during the Northridge earthquake of 1994 was as large as 1.18g (g is the gravitational acceleration) and the recorded ratio between the peak vertical and horizontal accelerations exceeded 1.5 [8]. During the Kobe earthquake of 1995, the downhole arrays installed at a reclaimed site recorded the peak ground acceleration in the vertical direction of being twice as high as the peak horizontal acceleration [9].

Keeping these observations in mind, great concern has arisen over the potential effect of vertical ground motion on engineering structures. To well address this emerging problem, the behaviour of site response to both vertical and horizontal earthquake motions needs to be investigated firstly. In this paper, a simple and practical procedure for this purpose is presented. The procedure uses the dynamic stiffness matrix method rather than the conventional recursive algorithm, and it retains the simplicity in nonlinear soil behaviour modelling through the equivalent-linear approach. The applicability of the procedure is evaluated against SHAKE in terms of horizontal site response and against downhole array records in terms of multi-directional site response.

2. Methodology and formulation

In real seismic environment, the ground motion amplification is very complicated. The amplification in either horizontal or vertical direction may be related to surface waves and the conversion between shear and compressional waves (e.g. [10,11]). Nevertheless, it has been well accepted in geotechnical analyses that the amplification of horizontal motion relates mainly to vertically propagating shear waves and the amplification of vertical motion relates mainly to vertically traveling compressional waves.

2.1. Response to horizontal earthquake motion

Consider vertically propagating shear waves in a viscoelastic soil layer (Fig. 1). The equation of motion is given by

$$\rho\frac{\partial^2 u}{\partial t^2}=G^*\frac{\partial^2 u}{\partial z^2} \tag{1}$$

where u is the horizontal displacement at depth z, ρ is the mass density of soil, and G^* represents the complex shear modulus, defined as $G^*=G(1+2i\zeta)$. Here ζ is known as the damping ratio.

Assuming steady-state harmonic waves with the frequency ω, the solution of Eq. (1) is readily given as

$$u(z,t)=(Ee^{ikz}+Fe^{-ikz})e^{i\omega t}=U(z,\omega)e^{i\omega t} \tag{2}$$

where the first term Ee^{ikz} represents the incident wave traveling in the negative z-direction (upward) and the second term Fe^{-ikz} represents the reflected wave traveling in the positive z-direction (downward). The parameter k is known as wave number given by $k=\sqrt{\rho\omega^2/G^*}$.

For a multi-layered soil–bedrock system shown in Fig. 1, the following recursive formulas can be established by using the above solution and considering the continuity conditions of displacements and tractions between layers m and m+1:

$$\begin{aligned}E_{m+1}&=\tfrac{1}{2}E_m(1+\alpha_m)e^{ik_mh_m}+\tfrac{1}{2}F_m(1-\alpha_m)e^{-ik_mh_m}\\F_{m+1}&=\tfrac{1}{2}E_m(1-\alpha_m)e^{ik_mh_m}+\tfrac{1}{2}F_m(1+\alpha_m)e^{-ik_mh_m}\end{aligned} \tag{3}$$

where h_m is the thickness of layer m and α_m the impedance ratio defined as $\alpha_m=\sqrt{(\rho_mG^*_m)/(\rho_{m+1}G^*_{m+1})}$.

The recursive procedure is started at the top free surface and then applied successively to layer m. The transfer function $TR_{m,n}$ relating the displacements at tops of layers m and n is defined as

$$TR_{m,n}(\omega)=\frac{U_m(\omega)}{U_n(\omega)} \tag{4}$$

The recursive formulation described above has been adopted in many programs for site response analysis (e.g. [3–5]).

Rather than using the recursive procedure, an alternative formulation involving the dynamic stiffness matrix [12,13] is used here. Referring to Fig. 1, the tractions at the top and bottom of layer m, T_m and T_{m+1}, can be given by

$$T_m=-G^*U_{m,z}(z_m=0),\quad T_{m+1}=G^*U_{m,z}(z_m=h_m) \tag{5}$$

The dynamic force–displacement relationship can then be established for layer m as

$$\begin{Bmatrix}T_m(\omega)\\T_{m+1}(\omega)\end{Bmatrix}=[S_m(\omega)]\begin{Bmatrix}U_m(\omega)\\U_{m+1}(\omega)\end{Bmatrix} \tag{6}$$

Here $[S_m(\omega)]$ is the dynamic stiffness matrix given by

$$[S_m(\omega)]=\begin{bmatrix}A_m & B_m\\B_m & A_m\end{bmatrix} \tag{7}$$

in which

$$A_m=\frac{\sqrt{\rho_mG^*_m}\omega}{\sin(k_mh_m)}\cos(k_mh_m),\quad B_m=-\frac{\sqrt{\rho_mG^*_m}\omega}{\sin(k_mh_m)} \tag{8}$$

By assembling the stiffness matrix of each layer, the total stiffness–displacement relationship for the layered system is

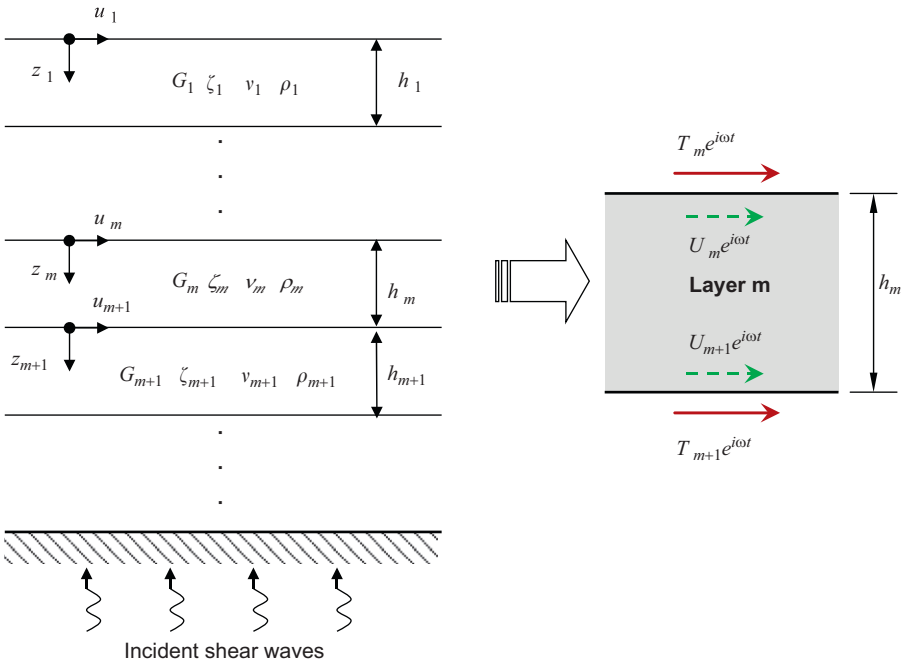

Fig. 1. Soil–bedrock system subjected to incident shear waves.

arrived

$$\begin{bmatrix} A_1 & B_1 & & & & & \\ B_1 & A_1+A_2 & B_2 & & & & \\ & B_2 & A_2+A_3 & B_3 & & & \\ & & B_3 & A_3+A_4 & & & \\ & & & & B_{n-3} & A_{n-3}+A_{n-2} & B_{n-2} \\ & & & & & B_{n-2} & A_{n-2}+A_{n-1} \end{bmatrix} \times \begin{Bmatrix} U_1 \\ U_2 \\ U_3 \\ U_4 \\ \\ U_{n-1} \\ U_n \end{Bmatrix} = \begin{Bmatrix} 0 \\ 0 \\ 0 \\ 0 \\ \\ 0 \\ 0 \end{Bmatrix} \quad (9)$$

2.2. Bedrock motion versus rock outcropping motion

To solve the equation, the earthquake motion input into the soil–bedrock system needs to be specified. As shown in Fig. 2, there are two ways to specify the input motion:

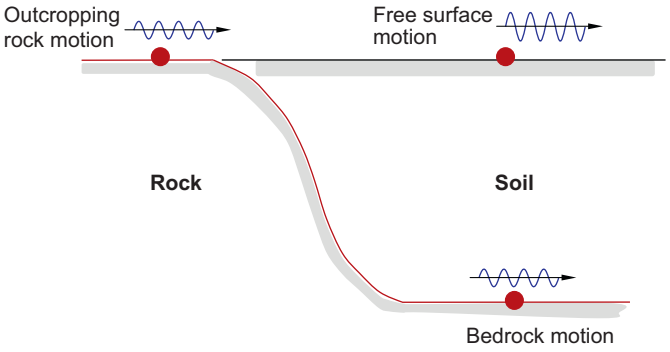

Fig. 2. Bedrock motion versus outcropping rock motion.

bedrock motion and rock outcropping motion. If the input motion is at the interface between the soil and bedrock, that is, given U_n, the motions in all layers can be computed directly from Eq. (9). If rock outcropping motion is given, however, a radiation dashpot with the damping coefficient of $\rho_{\text{rock}} v_{\text{srock}}$ [14] is introduced to radiate the energy from the soil to the bedrock. Here, ρ_{rock} and v_{srock} are the mass density and shear wave velocity of the rock. As a result, the displacement–force relationship becomes

$$\begin{bmatrix} A_1 & B_1 & & & & & \\ B_1 & A_1+A_2 & B_2 & & & & \\ & B_2 & A_2+A_3 & B_3 & & & \\ & & B_3 & A_3+A_4 & & & \\ & & & & B_{n-3} & A_{n-3}+A_{n-2} & B_{n-2} \\ & & & & & B_{n-2} & A_{n-2}+A_{n-1} \\ & & & & & & B_{n-1} \end{bmatrix} \begin{Bmatrix} B_{n-1} \\ A_{n-1}+S_n \end{Bmatrix} \begin{Bmatrix} U_1 \\ U_2 \\ U_3 \\ U_4 \\ \\ U_{n-1} \\ U_n \end{Bmatrix} = \begin{Bmatrix} 0 \\ 0 \\ 0 \\ 0 \\ \\ 0 \\ S_n U_c \end{Bmatrix} \quad (10)$$

where U_c is the displacement at the rock outcropping and $S_n = i\rho_{rock}v_{srock}\omega$. From Eq. (10) the motions in all layers can be solved subsequently.

2.3. Nonlinear soil behaviour

The nonlinear behaviour of soil, as illustrated in Fig. 3, has been well established in geotechnical engineering (e.g. [15–17]). To approximate the nonlinear response of a soil, a modulus reduction curve and a damping ratio curve need to be established and an equivalent-linear approach can be utilized. In this analysis, the strain vector obtained in the frequency domain is transformed into the time domain by using the inverse Fourier transformation. The maximum strain level is scaled by a factor (typically 0.65) to give an effective strain level, which is then used for the determination of the corresponding shear modulus and damping ratio for the next iteration. The process is repeated until the difference between the modulus reductions and damping ratios computed in two adjacent iterations is within an acceptable tolerance.

2.4. Response to vertical ground motion

The problem of vertical site response can be simplified with a one-dimensional wave propagation model involving vertical displacement w:

$$\rho\frac{\partial^2 w}{\partial t^2} = E_c\frac{\partial^2 w}{\partial z^2} + \tilde{\eta}\frac{\partial^3 w}{\partial z^2 \partial t} \tag{11}$$

where E_c is the constrained modulus and $\tilde{\eta}$ is the viscosity coefficient. They are defined, respectively, as

$$E_c = \frac{1-\upsilon}{(1+\upsilon)(1-2\upsilon)}E, \quad \tilde{\eta} = \frac{2E_c\tilde{\zeta}}{\omega} \tag{12}$$

where E is the Young's modulus, υ is the Poisson's ratio, and $\tilde{\zeta}$ is the damping ratio for vertical motion.

The solution of (11) has the form as

$$w(z,t) = (Ce^{i\tilde{k}z} + De^{-i\tilde{k}z})e^{i\omega t} = W(z,\omega)e^{i\omega t} \tag{13}$$

where the first term $Ce^{i\tilde{k}z}$ represents the incident wave traveling in the negative z-direction (upwards) and the second term $De^{-i\tilde{k}z}$ represents the reflected wave traveling in the positive z-direction (downwards). The parameter $\tilde{k}$ is wave number given by $\tilde{k} = \sqrt{\rho\omega^2/E_c^*}$, with the complex modulus $E_c^* = E_c(1+2i\tilde{\zeta})$.

Referring to Fig. 4, the force–displacement relationship for layer m can be established as

$$\begin{Bmatrix} N_m(\omega) \\ N_{m+1}(\omega) \end{Bmatrix} = [\tilde{S}_m(\omega)]\begin{Bmatrix} W_m(\omega) \\ W_{m+1}(\omega) \end{Bmatrix} \tag{14}$$

where

$$[\tilde{S}_m(\omega)] = \begin{bmatrix} \tilde{A}_m & \tilde{B}_m \\ \tilde{B}_m & \tilde{A}_m \end{bmatrix}$$

$$\tilde{A}_m = \frac{\sqrt{\rho_m E_{c_m}^*}\omega}{\sin(\tilde{k}_m h_m)}\cos(\tilde{k}_m h_m), \quad \tilde{B}_m = -\frac{\sqrt{\rho_m E_{c_m}^*}\omega}{\sin(\tilde{k}_m h_m)} \tag{15}$$

By assembling the stiffness matrix of each layer, the total stiffness–displacement relationship for the layered system is given by

$$\begin{bmatrix} \tilde{A}_1 & \tilde{B}_1 & & & & & \\ \tilde{B}_1 & \tilde{A}_1+\tilde{A}_2 & \tilde{B}_2 & & & & \\ & \tilde{B}_2 & \tilde{A}_2+\tilde{A}_3 & \tilde{B}_3 & & & \\ & & \tilde{B}_3 & \tilde{A}_3+\tilde{A}_4 & & & \\ & & & & \tilde{B}_{n-3} & \tilde{A}_{n-3}+\tilde{A}_{n-2} & \tilde{B}_{n-2} \\ & & & & & \tilde{B}_{n-2} & \tilde{A}_{n-2}+\tilde{A}_{n-1} & \tilde{B}_{n-1} \end{bmatrix} \times \begin{Bmatrix} W_1 \\ W_2 \\ W_3 \\ W_4 \\ \\ W_{n-1} \\ W_n \end{Bmatrix} = \begin{Bmatrix} 0 \\ 0 \\ 0 \\ 0 \\ \\ 0 \\ 0 \end{Bmatrix} \tag{16}$$

Similarly, if the input motion is specified at the interface between the soil and bedrock, then motions in all layers can be computed directly from Eq. (16). If given the outcropping vertical motion, a radiation dashpot with the damping coefficient of $\rho_{rock}v_{prock}$ is introduced to radiate the energy, where ρ_{rock} and v_{prock} are the mass density and compressional wave velocity of the rock. As a result, the response can be computed using the following matrix:

$$\begin{bmatrix} \tilde{A}_1 & \tilde{B}_1 & & & & & \\ \tilde{B}_1 & \tilde{A}_1+\tilde{A}_2 & \tilde{B}_2 & & & & \\ & \tilde{B}_2 & \tilde{A}_2+\tilde{A}_3 & \tilde{B}_3 & & & \\ & & \tilde{B}_3 & \tilde{A}_3+\tilde{A}_4 & & & \\ & & & & \tilde{B}_{n-3} & \tilde{A}_{n-3}+\tilde{A}_{n-2} & \tilde{B}_{n-2} \\ & & & & & \tilde{B}_{n-2} & \tilde{A}_{n-2}+\tilde{A}_{n-1} & \tilde{B}_{n-1} \\ & & & & & & \tilde{B}_{n-1} & \tilde{A}_{n-1}+\tilde{S}_n \end{bmatrix}$$

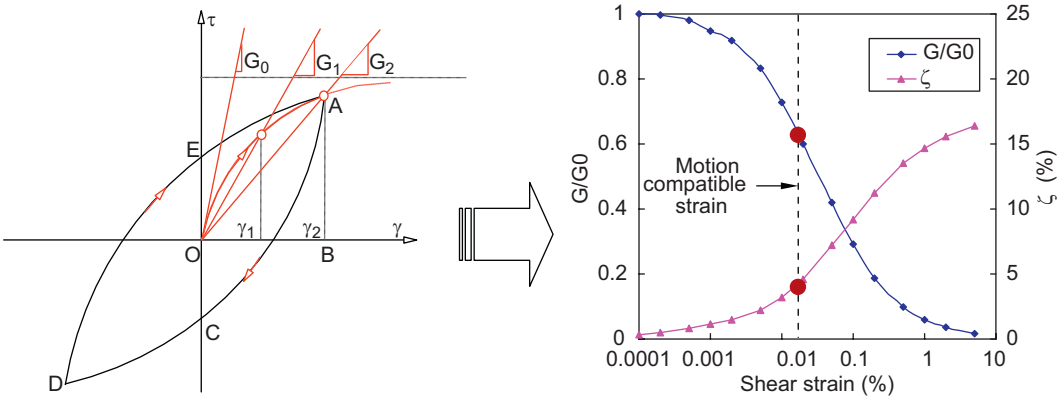

Fig. 3. Strain-dependent shear modulus and damping.

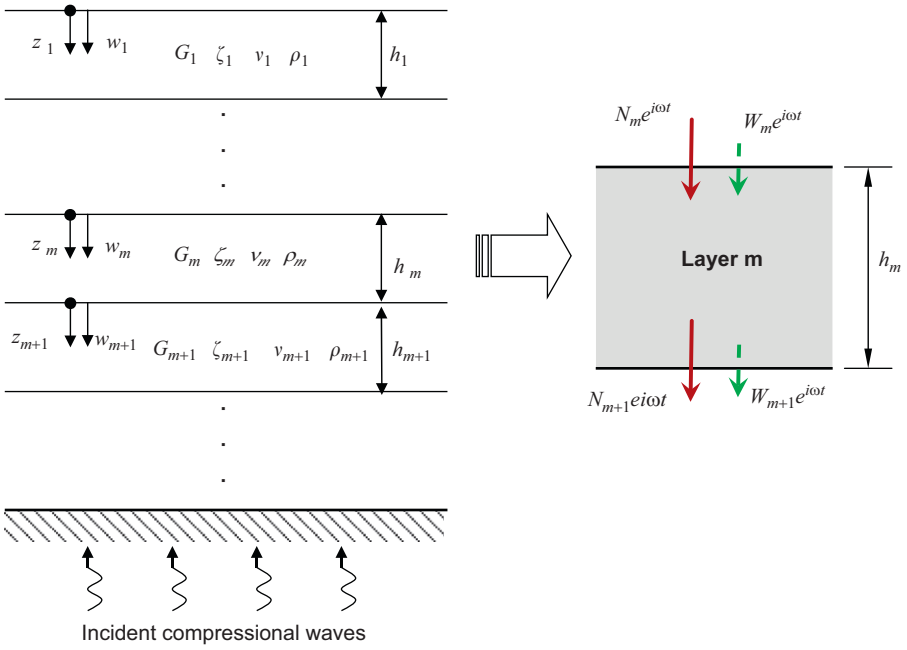

Fig. 4. Soil–bedrock system subjected to incident compressional waves.

$$\times \begin{Bmatrix} W_1 \\ W_2 \\ W_3 \\ W_4 \\ \\ \\ W_{n-1} \\ W_n \end{Bmatrix} = \begin{Bmatrix} 0 \\ 0 \\ 0 \\ 0 \\ \\ \\ 0 \\ \tilde{S}_n W_c \end{Bmatrix} \tag{17}$$

where W_c is the displacement at the rock outcropping and $\tilde{S}_n = \mathrm{i}\rho_{\mathrm{rock}} v_{\mathrm{prock}} \omega$.

2.5. Degradation of constrained modulus

While it has been widely accepted that the shear modulus and damping ratio are shear strain dependent, laboratory test data for the constrained modulus and the damping ratio of compressional waves is scarce. Here, the assumption of constant Poisson's ratio is introduced such that the degraded shear modulus and shear wave velocity can be transformed to constrained modulus and compressional wave velocity through the following relationship:

$$v_{\mathrm{p}} = \sqrt{\frac{E_{\mathrm{c}}}{\rho}} = \sqrt{\frac{2(1-\upsilon)}{1-2\upsilon}} v_{\mathrm{s}} \tag{18}$$

As for the damping ratio of vertical motion, current understanding is even limited. For the first instance, it is assumed to take the same value of the damping ratio yielded from the horizontal site response analysis.

3. Procedure validation

A computer programme named PASS has been developed based on the formulation outlined above [18]. The programme is built in the modern MATLAB environment so as to take full advantages of the matrix operations in MATLAB.

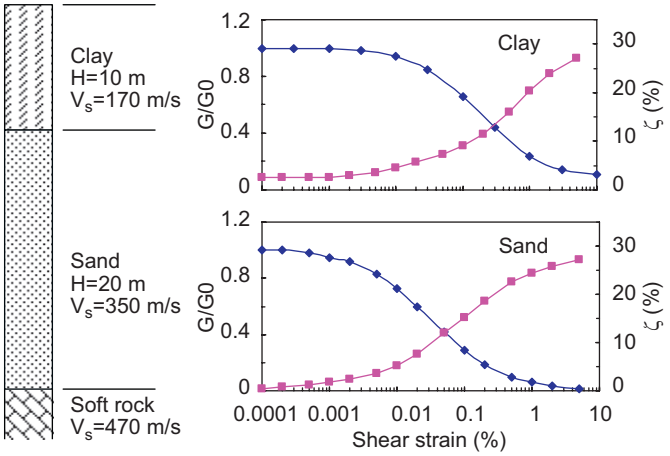

Fig. 5. Hypothesized site for validation.

3.1. Comparison with SHAKE

Firstly the reliability and accuracy of PASS as compared with SHAKE in terms of horizontal site response needs to be assessed. Fig. 5 shows a hypothesized soil site for the purpose of assessment. It comprises a top clay layer of 10 m and an underlying sand layer of 20 m. The shear wave velocities of the clay and sand are 170 and 350 m/s, respectively, and the site can be classified as stiff-soil site (S_{D} type) according to the UBC site classification system. The shear modulus reduction curve and damping curve suggested by Seed and Idriss [15] for sand are employed to represent the sand behaviour, whereas the modulus reduction and damping curves used here for the clay are taken from the proposal of Sun et al. [17].

The transfer function of the site for the horizontal motion is computed using PASS and SHAKE91, respectively, and the results are compared in Fig. 6. In the computation, the soil is assumed either to be elastic or viscoelastic with the damping ratio of 5% and 10%, respectively. It is clear that the results produced by PASS are in good agreement with those by SHAKE. Both programs

predict the fundamental site frequency of about 2.62 Hz for the two-layer site. The motion amplitude at the ground surface is amplified when seismic waves travel from the base to the surface and the magnitude of amplification decreases with increasing damping.

Fig. 7 shows the ratio between base motion amplitude and outcropping motion amplitude as a function of frequency. Note that SHAKE calculates the spectral ratio based on the following analytical transfer function:

$$\mathrm{TR}_{m,n}(\omega) = \frac{E_n(\omega) + F_n(\omega)}{2E_n(\omega)} \tag{19}$$

Here $2E_n(\omega)$ indicates that the incident waves are identical with the reflected waves at the rock outcropping. In PASS, however, the spectral ratio is evaluated directly based on Eq. (10). The comparison shown in Fig. 7 shows the reliability and accuracy of PASS in handling the outcropping rock motion. The base motion amplitude, compared with the outcropping motion amplitude, is reduced at frequencies between site frequencies and this reduction is dependent on the damping. At zero damping the base motion amplitude becomes zero at site frequencies.

Now, consider the nonlinear response of the two-layer site subjected to horizontal earthquake shaking. The time histories of the input motion are shown in Fig. 8, which is the east–west component of the acceleration recorded at the Diamond Heights rock station during the 1989 Loma Prieta earthquake. The peak acceleration of this record is 0.113 g. The input motion is specified at rock outcropping. The acceleration time histories at the ground surface computed using PASS and SHAKE are compared in the top two plots in Fig. 8. Fig. 9 presents the time histories of shear stress and shear strain at the depth of 15 m from PASS and SHAKE. Again, it is observed that the difference between the results produced by PASS and SHAKE is negligible. The good agreement is also

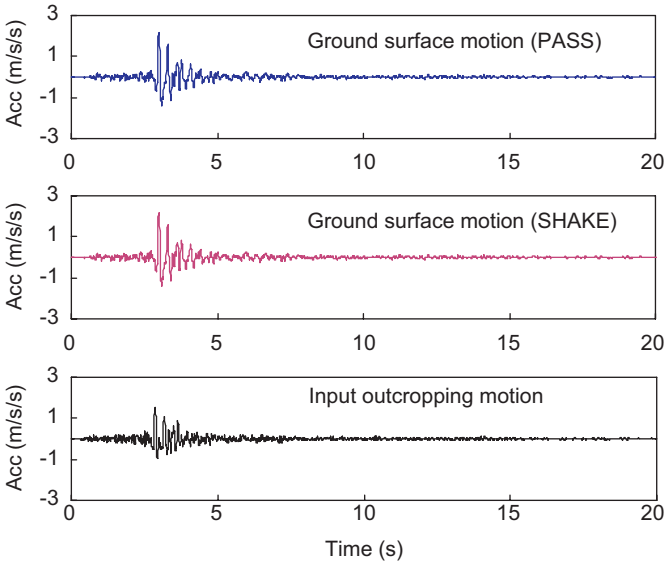

Fig. 8. Input horizontal motion and computed ground surface motion.

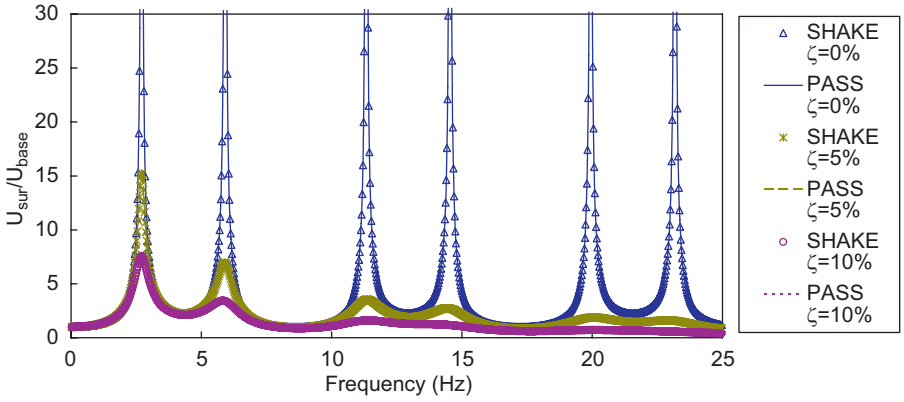

Fig. 6. Spectral ratio between surface motion and base motion.

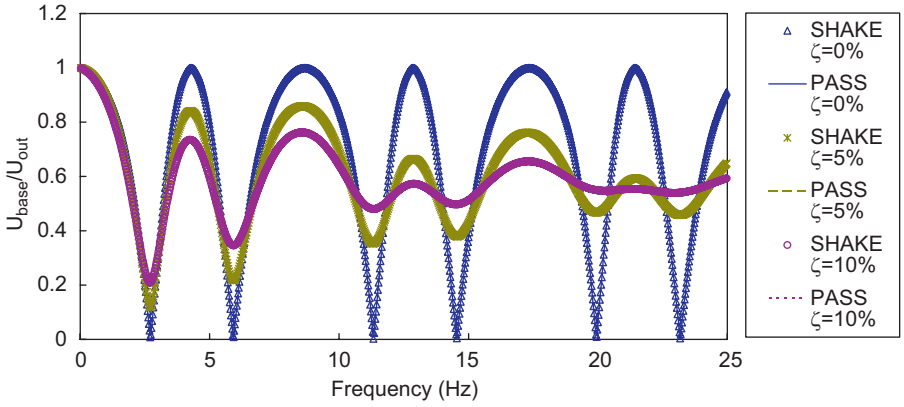

Fig. 7. Spectral ratio between base motion and outcropping motion.

observed in Fig. 10 where the distributions with depth of the shear strain, shear modulus reduction and damping ratio are presented. An alternative comparison is given in Table 1, which gives values of the peak shear strain, peak shear stress and degraded shear modulus at various depths. Note that the iteration number required by PASS is 5 as compared with the iteration number 8 required by SHAKE.

The major differences in the numerical implementation of the program PASS and SHAKE91 can be summarised as follows:

(a) PASS assembles a dynamic stiffness matrix for the layered soil–rock system to compute the response and avoid the use of the recursive algorithm in SHAKE91. The responses of all layers are solved at one running. In SHAKE91, however, the user needs to specify beforehand the layers for which their responses need to be computed.

(b) PASS is developed in the modern MATLAB environment. It uses a different fast Fourier transform (FFT) routine. The routine computes the discrete Fourier transform (DFT) in one or more dimensions, of arbitrary input size, and of both real and complex data. This allows less restriction for the earthquake input motion than SHAKE91.

(c) PASS uses a more efficient and robust procedure to iterate toward strain compatible soil properties, whereas in SHAKE91 the user has to specify the iteration number beforehand. The last iteration required to drop the modulus and damping error within the specified error tolerance in PASS generally produces smaller final errors than the last iteration for the same error tolerance in SHAKE91.

3.2. *Verification using downhole array records*

The downhole array records obtained at the Turkey Flat test site in California are used in the validation. The test site is at Parkfield which lies along the segment of the San Andreas Fault [19]. The sediments in the site are comprised mainly of the silty clays and clayey sands. Strong seismographs were installed in a borehole in the valley center of the site (Fig. 11). The simplified soil profile at the borehole location, based on a comprehensive site investigation programme [19], is shown in Fig. 12. The top layer consists of dark brown silty clay of about 2.4 m and the underlying layer consists of primarily clayey sand

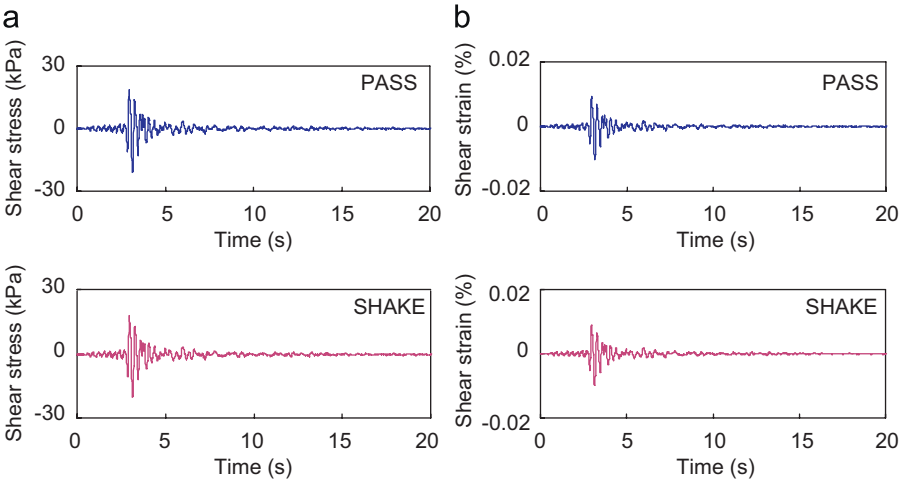

Fig. 9. Computed time histories of (a) stresses and (b) strains at depth of 15 m.

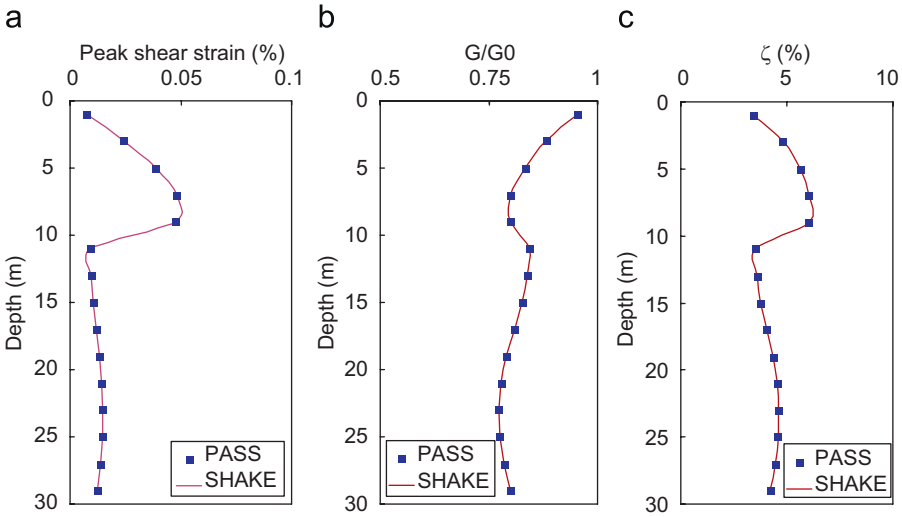

Fig. 10. Computed profiles of (a) peak shear strain, (b) shear modulus reduction and (c) damping ratio.

Table 1
Comparison of results from PASS and SHAKE

Depth (m)	Peak shear strain (%)			Shear modulus (kPa)			Peak shear stress (kPa)		
	SHAKE	PASS	RD (%)	SHAKE	PASS	RD (%)	SHAKE	PASS	RD (%)
1	0.00778	0.00774	−0.5	49,600.4	49,614.0	0.0	3.86	3.84	−0.5
3	0.02423	0.02408	−0.6	45,811.1	45,842.0	0.1	11.10	11.04	−0.6
5	0.03886	0.03861	−0.6	43,328.8	43,363.0	0.1	16.84	16.74	−0.6
7	0.04816	0.04775	−0.9	41,531.5	41,608.0	0.2	20.00	19.87	−0.7
9	0.04779	0.04753	−0.5	41,601.5	41,650.0	0.1	19.88	19.80	−0.4
11	0.00877	0.00877	0.0	206,818.4	206,830.0	0.0	18.14	18.14	0.0
13	0.00927	0.00927	0.0	205,555.4	205,560.0	0.0	19.05	19.06	0.0
15	0.01037	0.01037	0.0	202,502.0	202,510.0	0.0	21.00	21.00	0.0
17	0.01175	0.01175	0.0	197,962.4	197,970.0	0.0	23.26	23.26	0.0
19	0.01324	0.01323	−0.1	193,622.1	193,660.0	0.0	25.64	25.62	−0.1
21	0.01437	0.01435	−0.1	190,634.2	190,690.0	0.0	27.39	27.36	−0.1
23	0.01487	0.01485	−0.1	189,384.1	189,440.0	0.0	28.16	28.13	−0.1
25	0.01462	0.01461	−0.1	190,023.1	190,040.0	0.0	27.78	27.76	−0.1
27	0.01383	0.01382	−0.1	192,045.8	192,050.0	0.0	26.56	26.54	−0.1
29	0.01242	0.01243	0.1	195,949.8	195,920.0	0.0	24.34	24.35	0.1

Note 1: RD (relative difference) = (PASS/SHAKE)−1 (in percent).
Note 2: Iteration number of SHAKE = 8; Iteration number of PASS = 5.

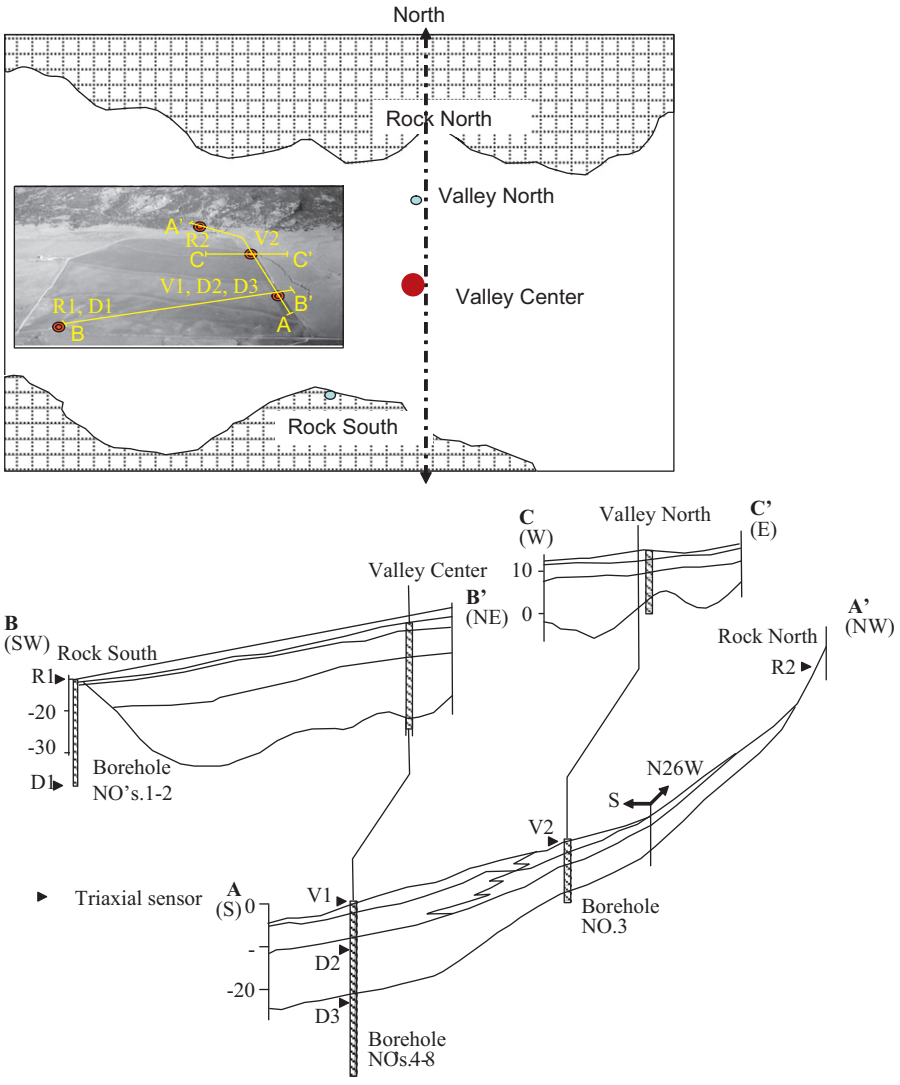

Fig. 11. Plan and section view of Turkey Flat test site (after [19]).

having higher concentrations of sandy clay and gravel. The mass densities of the silty clay and the clayey sand are 1500 and 1900 kg/m^3, respectively. The shear wave velocity increases from 135 m/s in the silty clay to 460 and 610 m/s in the clayey sand. The compressional wave velocity varies from 320 in the top layer to 970 m/s in the bottom layer. The site can be classified as the shallow stiff-soil site (Table 2).

The site was subjected to an earthquake on September 28, 2004 and the time histories of accelerations were successfully recorded at the surface and depths. In this study, the accelerations in the east–west and up–down directions recorded by the accelerometer at the depth of 11 m are used as the bedrock input motions (see Fig. 13). The shear modulus reduction curve proposed by Sun et al. [17] for clay with the plasticity index between 20 and 40 is assumed to approximately represent the nonlinear behaviour of the soils at the site (Fig. 12). The attenuation properties of the soils measured using field seismic methods [19] showed a significant scatter, but basically

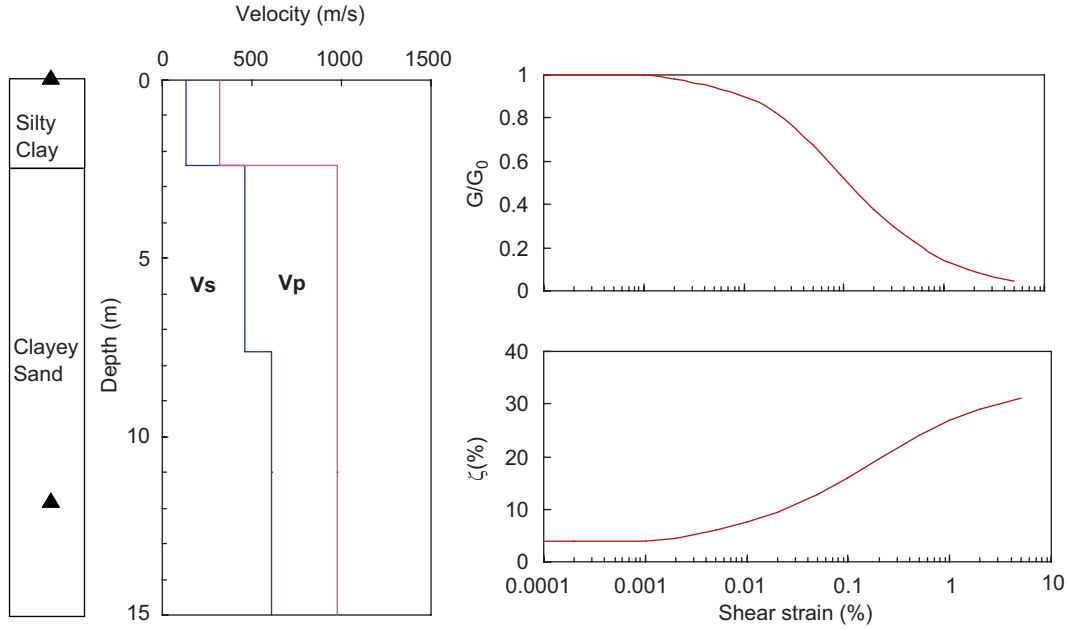

Fig. 12. Soil profile of Turkey Flat test site.

Table 2
Properties of soils at Turkey Flat test site (after [19])

Layer	Depth (m)	Soil description	Shear wave velocity (m/s)	Compressional wave velocity (m/s)	Mass density (kg/m^3)	Poisson's ratio
1	0–2.4	CL	135	320	1500	0.3917
2	2.4–7.6	SC	460	975	1800	0.3568
3	7.6–11	SC	610	975	1900	0.1784

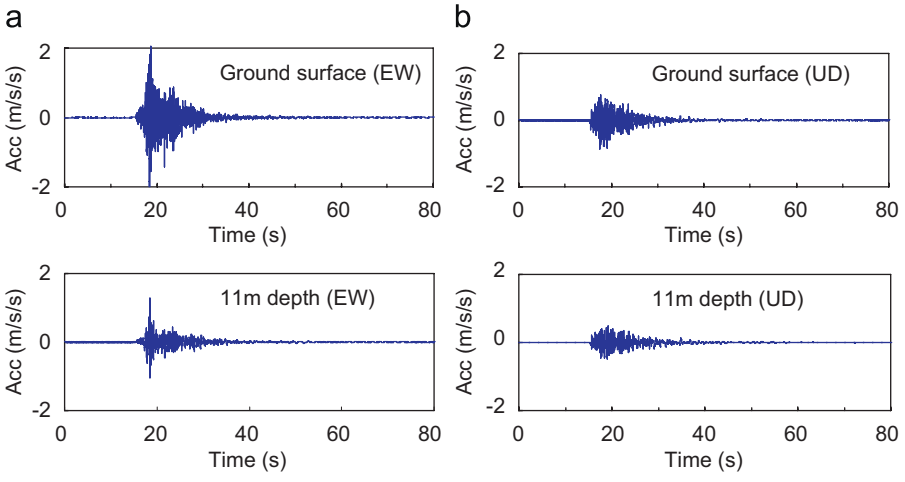

Fig. 13. Ground motion records: (a) horizontal and (b) vertical.

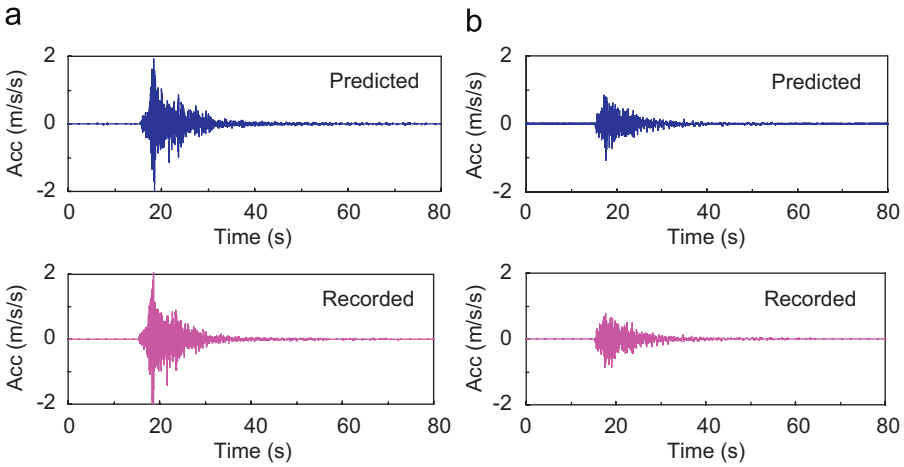

Fig. 14. Predicted and recorded ground motions at surface: (a) horizontal and (b) vertical.

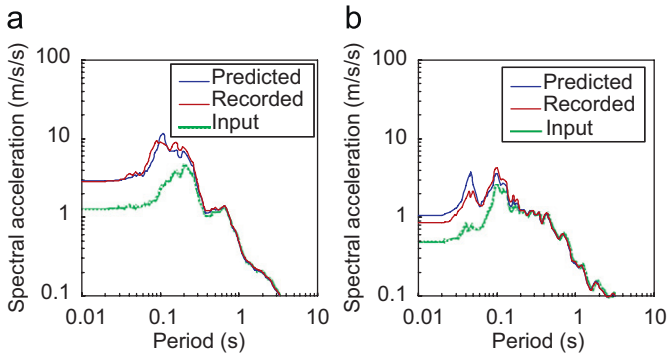

Fig. 15. Predicted and recorded spectral accelerations: (a) horizontal and (b) vertical.

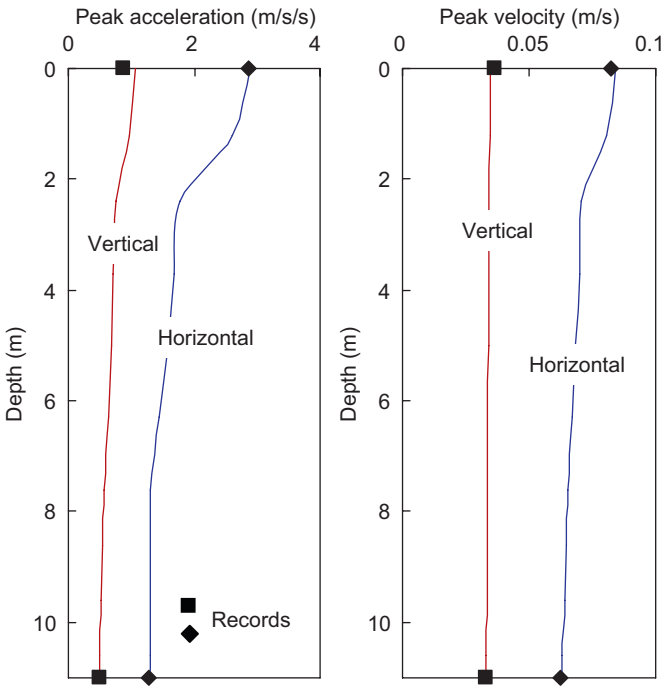

Fig. 16. Predicted distributions of peak acceleration and velocity with depth.

showed high values. For example, the measured damping ratio of shear waves in shallow soils ranges from as low as 5% to as large as 30%, and these values are for frequencies between 25 and 70 Hz. For simplicity, the upper bound damping ratio curve proposed by Sun et al. [17] for clay soil is used here (Fig. 12).

In Fig. 14, the time histories of the ground surface accelerations in both horizontal and vertical components computed by PASS are compared with the records. A fairly good agreement is obtained for both components. This agreement is also observed in the response spectra shown in Fig. 15. Fig. 16 shows the distributions with depth of peak accelerations and velocities in both components superposed with the recorded values. The accuracy of these predictions produced by PASS appears to be acceptable. The calculated time histories of shear stress and shear strain at various depths are shown in Figs. 17 and 18 presents the predicted time histories of normal stress and normal strain at different depths. This information is useful in the analysis of underground structures and liquefaction potential assessment.

4. Concluding remarks

Current practice in earthquake ground response has tended to focus on the horizontal motion and simply disregard the vertical motion. Aimed at addressing an emerging problem on the effects of vertical ground motion, a simple and practical procedure has been presented in this paper for the analysis of site response to both horizontal and vertical earthquake motions. The procedure uses the dynamic stiffness matrix method rather than the conventional recursive algorithm, and retains the simplicity in nonlinear soil behaviour modelling through the equivalent-linear approach. The assumption of constant Poisson's ratio is introduced to derive the degraded constrained modulus for vertical site response, and the damping ratio of the vertical motion is assumed to be the same with that yielded from the horizontal site response. The procedure can handle both the bedrock and rock outcropping input motions and for the latter case viscous dampers are employed to radiate the energy of seismic waves. The detailed assessment of the procedure indicates that it is able to produce reasonable predictions for both horizontal and vertical responses.

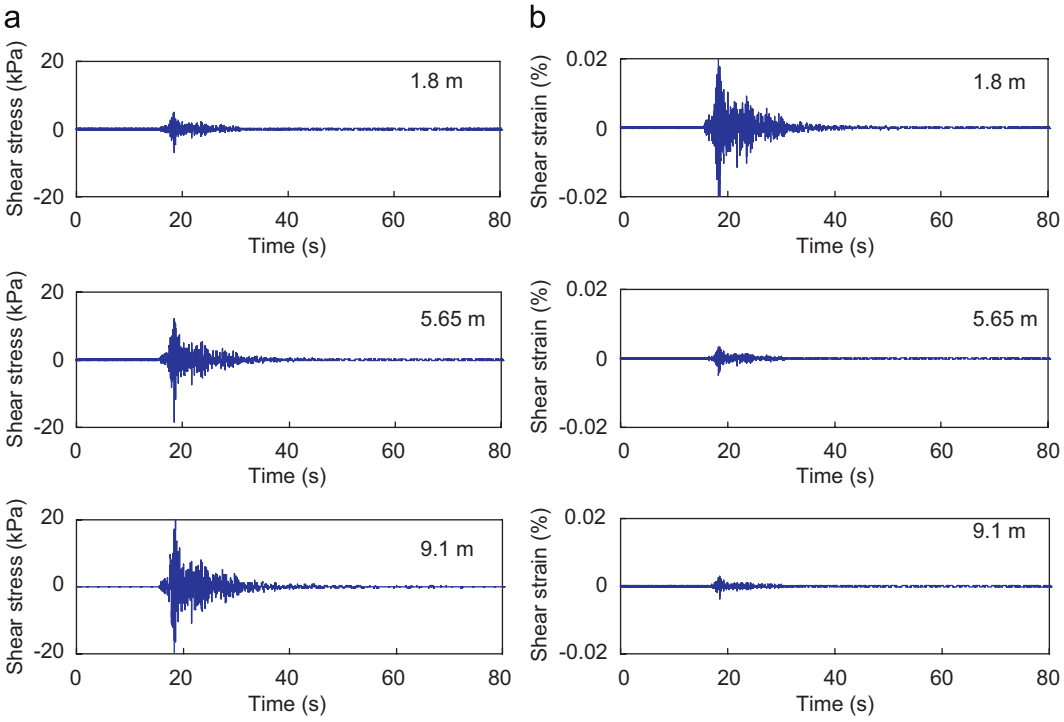

Fig. 17. Predicted time histories of (a) shear stresses and (b) shear strains at different depths.

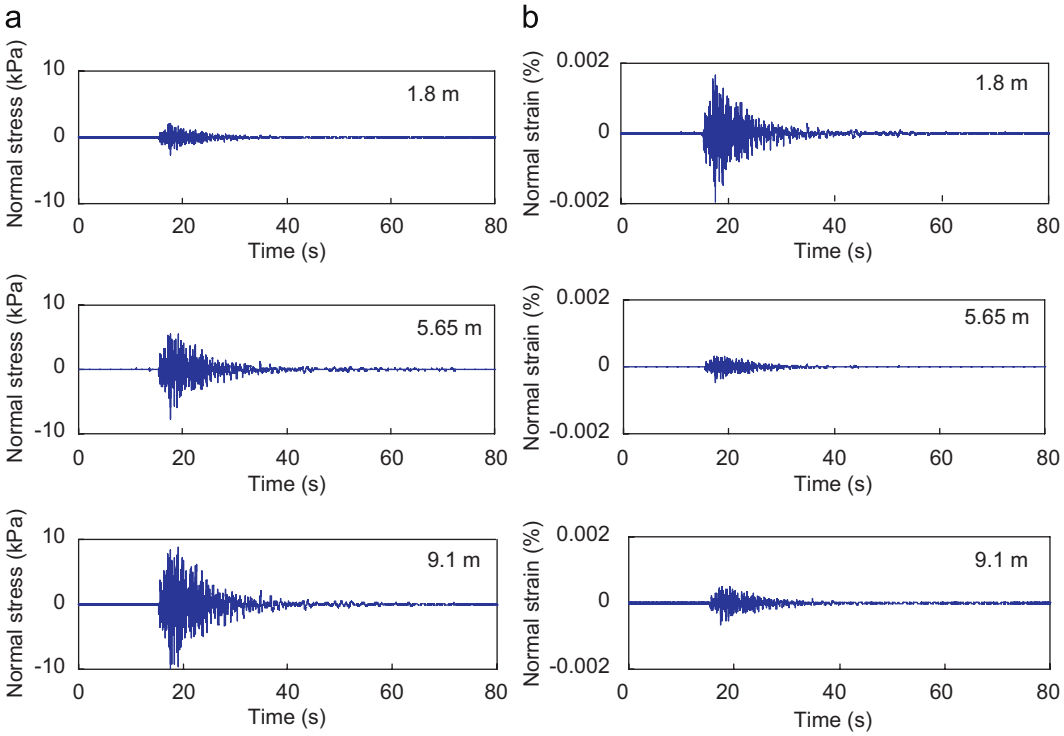

Fig. 18. Predicted time histories of (a) normal stresses and (b) normal strains at different depths.

Acknowledgements

The work described in this paper was supported by the Research Grants Council of Hong Kong (HKU7127/04E and HKU7191/05E). This support is gratefully acknowledged. The authors thank the California Department of Conservation Division of Mines and Geology and the Pacific Earthquake Engineering Research Center in California for making useful information available for this study.

References

[1] Schnabel PB, Lysmer J, Seed HB. SHAKE: a computer program for earthquake response analysis of horizontally layered sites. Report EERC 72-12. Berkeley: Earthquake Engineering Research Center, University of California; 1972.

[2] Arulanandan K, Scott RF, editors. VELACS: verification of numerical procedures for the analysis of soil liquefaction problems. Rotterdam: A.A. Balkema; 1993.

[3] Idriss IM, Sun JI. User's manual for SHAKE91. Davis: Department of Civil and Environment Engineering, University of California; 1992.

[4] Bardet JP, Ichii K, Lin CH. EERA: a computer program for equivalent-linear earthquake site response analyses of layered soil deposits. Department of Civil Engineering, University of Southern California, 2000.

[5] ProShake. Ground response analysis program—user's manual. EduPro Civil Systems, Inc., 1998.

[6] UBC. Uniform building code. International Conference of Building Officials, Whittier, California, 1997.

[7] Day RW. Geotechnical earthquake engineering handbook. New York: McGraw-Hill; 2002.

[8] NCEER. FHWA/NCEER workshop on national representation of seismic ground motion for new and existing highway facilities. Technical report, NCEER-97-0010. Buffalo, New York: National Center for Earthquake Engineering, Research; 1997.

[9] Yang J, Sato T. Interpretation of seismic vertical amplification observed at an array site. Bull Seismol Soc Am 2000;90(2):275–85.

[10] Yang J. Saturation effects on horizontal and vertical motions in a layered soil–bedrock system due to inclined SV waves. Soil Dyn Earthquake Eng 2001;21(6):527–36.

[11] Yang J. Frequency-dependent amplification of unsaturated surface soil layer. J Geotech Geoenviron Eng—ASCE 2006;132(4):526–31.

[12] Kausel E, Roesset JM. Stiffness matrices for layered soils. Bull Seismol Soc Am 1981;71(6):1743–61.

[13] Wolf JP. Foundation vibration analysis using simple physical models. Englewood Cliffs, NJ: Prentice-Hall; 1994.

[14] Lysmer J, Kuhlemeyer RL. Finite dynamic model for infinite media. J Eng Mech Div—ASCE 1969;95(1):859–77.

[15] Seed HB, Idriss IM. Soil moduli and damping factors for dynamic response analyses. Report EERC 70-10. Berkeley: Earthquake Engineering Research Center, University of California; 1970.

[16] Vucetic M, Dobry R. Effect of soil plasticity on cyclic response. J Geotech Eng—ASCE 1991;117(1):89–107.

[17] Sun JI, Golesorkhi R, Seed HB. Dynamic Moduli and damping ratios for cohesive soils. Report UCB/EERC 88/15. Berkeley: Earthquake Engineering Research Center, University of California; 1988.

[18] Yang J, Yan XR. PASS: a computer program for practical analysis of layered soil–rock systems. Department of Civil Engineering, The University of Hong Kong, 2006.

[19] Real CR. Turkey Flat, USA site effects test area: site characterization (Report 2). Technical report no. 88-2. California: California Department of Conservation Division of Mines and Geology; 1988.